EurJIC
European Journal of Inorganic Chemistry

Research Article
doi.org/10.1002/ejic.202400422

Chemistry Europe
European Chemical Societies Publishing

www.eurjic.org

Single-Electron Oxidation, Chloride Abstraction, and Hydride-Induced Decomposition of a Dichloro-Bis(Germylene)

Yiyi He,[a] Cauê P. Souza,[b] Jonas Weiser,[c] Maximilian Dietz,[d, e] Ivo Krummenacher,[d, e] Rian D. Dewhurst,[d, e] Holger Braunschweig,*[d, e] Felipe Fantuzzi,*[b] and Jingjing Cui*[a]

In this work we explore the reactivity of a dichloro-bis(germylene) compound that features a naphthyridine diimine (NDI) ligand, denoted NDI-Ge_2Cl_2. Upon reaction with the oxidant $[Cp_2Fe][BAr^F_4]$ ($Cp{=}C_5H_5$, $BAr^F_4 = [\{3,5\text{-}(CF_3)_2C_6H_3\}_4B]$), we observed the formation of the radical species $[NDI\text{-}Ge_2Cl_2]^{\bullet+}$ $[BAr^F_4]^-$. Furthermore, the introduction of $Na[BAr^F_4]$ induced a single chloride anion abstraction process, resulting in the formation of $[NDI\text{-}Ge_2Cl][BAr^F_4]$. The addition of $Li[HB(^sBu)_3]$ to NDI-Ge_2Cl_2 led to the generation of NDI–Ge, presumably via a Cl/H exchange pathway followed by a decomposition process.

Introduction

Germylenes, heavier analogs of carbenes, exhibit diverse reactivities, including oxidation, reduction, coordination to Lewis acids or bases, and activation of small molecules.[1] In the case of germylenes featuring a Ge–X (X = halogen) bond, further derivations, such as nucleophilic substitution, halogen extraction, and halogen/H exchange, become conceivable.[1a,f,2] However, the exploration of dihalo-digermylenes (Figure 1, I–**III**) and their reactivity is rather limited, with a predominant focus on their reduction chemistry.[3] The contribution from the Rivard group[4] represents a rare example of a detailed investigation into the derivation of dichloro-digermylene, providing invaluable insights into this specific class of compounds. This situation is in sharp contrast to the extensive reactivity studies on halo-monogermylenes.

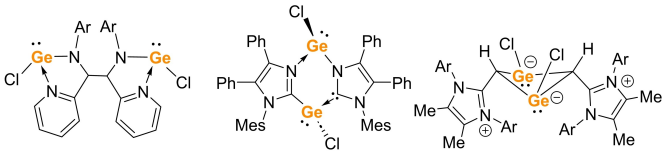

Figure 1. Structurally characterized dihalo-digermylenes (Ar = 2,6-diisopropylphenyl, Mes = 2,4,6-trimethylphenyl).

Recently, utilizing a redox-active naphthyridine – diimine ligand (NDI) (Figure 2, **IV**), we successfully synthesized dichloro-digermylene **1** (NDI-Ge_2Cl_2) and subsequently obtained a six-electron donating digermylene NDI-Ge_2 (**V**) via the reduction of **1**. Additionally, we achieved the salt elimination of **1** by employing a transition-metal-based nucleophile.[5] In this work, we demonstrate single-electron oxidation, chloride anion abstraction, halogen/H exchange, and subsequent disproportionation of compound **1**.

Results and Discussion

Upon the addition of equimolar amounts of oxidant $[Cp_2Fe][BAr^F_4]$ ($Cp{=}C_5H_5$, $BAr^F_4 = [\{3,5\text{-}(CF_3)_2C_6H_3\}_4B]$) to a C_6D_6 solution of **1** at ambient temperature, the appearance of the reaction mixture remained unchanged. However, the ^1H NMR spectrum exclusively exhibited a signal for Cp_2Fe, suggesting the formation of radical species **2** (Scheme 1).

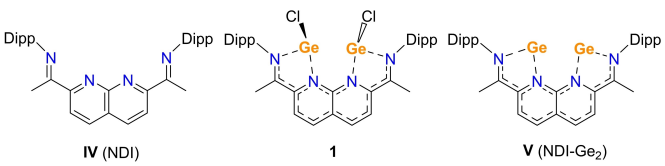

Figure 2. Structures of **IV**, **V** and **1** (Dipp = 2,6-diisopropylphenyl).

[a] *Y. He, J. Cui*
School of Chemistry and Environmental Engineering, Wuhan Institute of Technology, Wuhan 430205, P.R. China
E-mail: 17061701@wit.edu.cn

[b] *C. P. Souza, F. Fantuzzi*
School of Chemistry and Forensic Science, University of Kent, Park Wood Rd, Canterbury CT2 7NH, UK
E-mail: f.fantuzzi@kent.ac.uk

[c] *J. Weiser*
Institute for Physical and Theoretical Chemistry, Julius-Maximilians-Universität Würzburg, Emil-Fischer-Str. 42, 97074 Würzburg, Germany

[d] *M. Dietz, I. Krummenacher, R. D. Dewhurst, H. Braunschweig*
Institute for Inorganic Chemistry, Julius-Maximilians-Universität Würzburg, Am Hubland, 97074 Würzburg, Germany
E-mail: h.braunschweig@uni-wuerzburg.de

[e] *M. Dietz, I. Krummenacher, R. D. Dewhurst, H. Braunschweig*
Institute for Sustainable Chemistry & Catalysis with Boron, Julius-Maximilians-Universität Würzburg, Am Hubland, 97074 Würzburg, Germany

Supporting information for this article is available on the WWW under https://doi.org/10.1002/ejic.202400422

Research Article
doi.org/10.1002/ejic.202400422

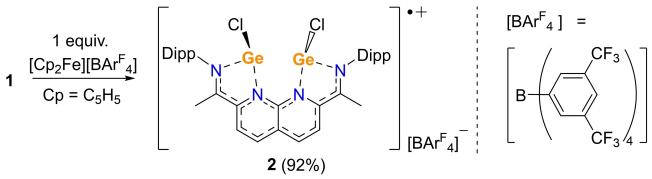

Scheme 1. Synthesis of compound **2** (Dipp = 2,6-diisopropylphenyl).

After removing Cp_2Fe by hexane washing in an ultrasound bath, single crystals suitable for X-ray diffraction analysis were obtained. The structure of the cationic part of **2** (Figure 3) strongly resembles that of **1**.[6] The mean planes of the two $C_2N_4Ge_2$ moieties display a slightly smaller dihedral angle of 11.70° compared to that observed in **1** (15.86°),[5] indicating a distorted arrangement of the naphthyridine-diimine-Ge_2 unit. The distance between the two Ge atoms increased from 2.8944(9) Å in **1** to 3.0021(15) Å in **2**. The Ge–Cl bonds [2.2218(18) and 2.2424(15) Å], the Ge–N bonds [2.015(3)–2.049(4) Å] and the sum of the bond angles (268.37°–270.34°) around the Ge atoms are all comparable to those of **1** [Ge–Cl bond 2.2916(7) Å, Ge–N bonds 1.9663(15) and 2.0011(16) Å, and the bond angle sum of Ge 273.11(15)°]. Adding two equivalents of [Fc][BAr^F_4] to **1** led to the same result, even with heating to 90 °C.

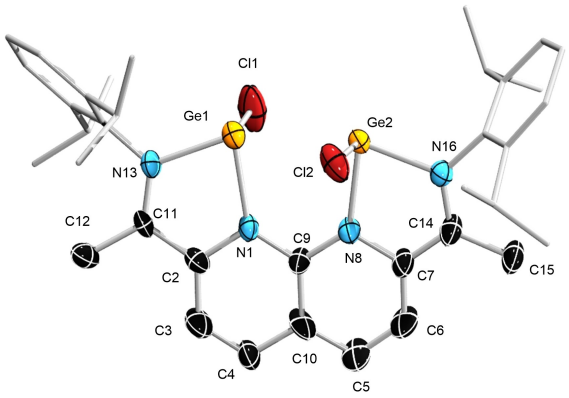

Figure 3. Solid-state structure of the cation of **2** (hydrogen atoms and ellipsoids of the Dipp groups are omitted for clarity). Thermal ellipsoids are set at the 50% probability level. Selected bond lengths [Å] and angles [°]: Ge1…Ge2, 3.001(2); Ge1–Cl1, 2.2424(15); Ge1–N1, 2.049(4); Ge1–N13, 2.015(3); Ge2–Cl2, 2.2218(18); Ge2–N8, 2.044(4); Ge2–N16, 2.020(3); C2–C11, 1.429(6); C7–C14, 1.442(6); Cl1–Ge1–N1, 95.91(11); Cl1–Ge1–N13, 92.55(11); N1–Ge1–N13, 79.92(13); Cl2–Ge2–N8, 94.78(11); Cl2–Ge2–N16, 95.41(11); N8–Ge2–N16, 80.17(13).

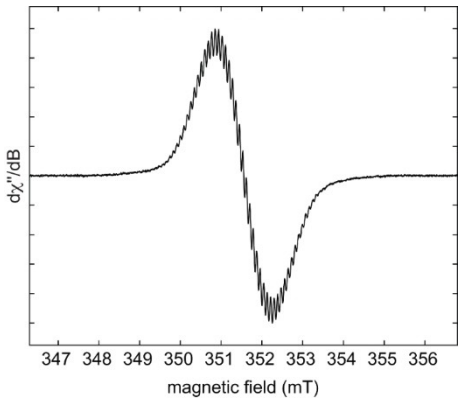

Figure 4. Experimental continuous-wave (CW) X-band EPR spectrum of **2** in toluene at room temperature. Experimental parameters: microwave frequency = 9.86 GHz; microwave power = 2 mW; modulation amplitude = 0.2 G; conversion time = 40 ms; modulation frequency = 100 kHz.

The electron paramagnetic resonance (EPR) spectrum of a toluene solution of compound **2** at room temperature exhibited a single broad peak ($g = 2.0029$) with a peak-to-peak linewidth of 1.4 mT (Figure 4). Simulating the spectrum is unfeasible due to complicated overlapping couplings that are difficult to resolve. For a better understanding of the radical cation [NDI-Ge_2Cl_2]$^{\bullet+}$, we performed DFT calculations at the M06-D3/def2-SVP level of theory.[7] We selected this level based on our preliminary benchmark investigation, as it yielded the most accurate structural agreement with the available experimental X-ray data.[5,8] The canonical Kohn–Sham singly-occupied molecular orbital (SOMO, Figure 5A) indicates a delocalization of the radical electron via the NDI ligand instead of the Ge atoms, in agreement with the experimental findings. Additional analysis of the spin density (Figure 5B) corroborated this conclusion. The positive charge is evenly distributed and is localized on the Ge atoms, each possessing a Mulliken charge of 0.64.

The combined information from the EPR study and the DFT calculations suggested that the radical predominantly localizes on the ligand rather than on the Ge atoms, as observed previously for [(dpp-BIAN)GeCl]$^{\bullet+}$[$GeCl_3$]$^-$ (dpp-BIAN = 1,2-Bis{(2,6-di*iso*propyl-phenyl)imino}acenaphthene) (Figure 6, **VI**),[9] 2,6-diiminophenyl-supported germylidendiide dianion radical **VII**,[10] β-diketiminato germanium radical complex $^{\bullet}$LGe ($^{\bullet}$L = $^{\bullet}$[PhC(PhCN-Dipp)$_2$]$_2^-$) (**VIII**),[11] the dipyrromethene-based neutral radical **IX**,[12] and the open-shell germylene stabilized by a phenalenyl-based bidentate ligand **X**.[13]

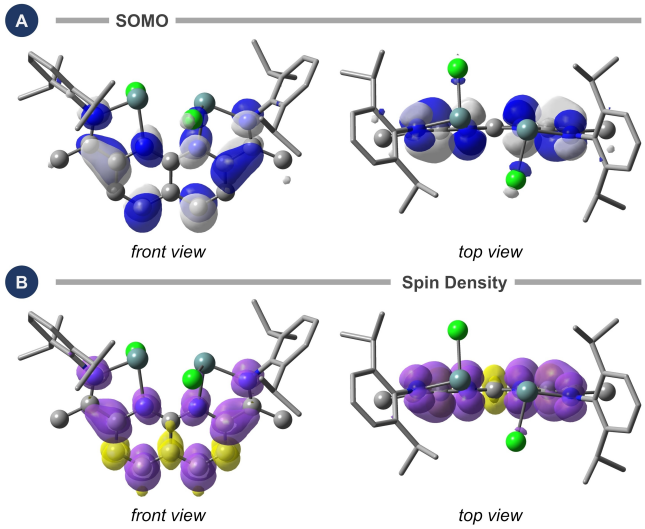

Figure 5. (A) Kohn–Sham SOMO (isovalue: 0.03) and (B) total spin density (isovalue: 0.015) of compound **2**. Hydrogen atoms are omitted for clarity. Level of theory: M06-D3/def2-SVP.

Research Article
doi.org/10.1002/ejic.202400422

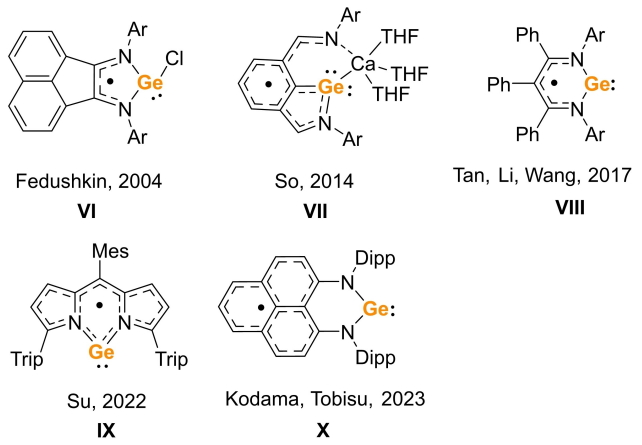

Figure 6. Structurally characterized delocalized germanium radicals (Ar = 2,6-diisopropylphenyl, Mes = 2,4,6-trimethylphenyl, Trip = 2,4,6-triisopropylphenyl, Dipp = 2,6-diisopropylphenyl).

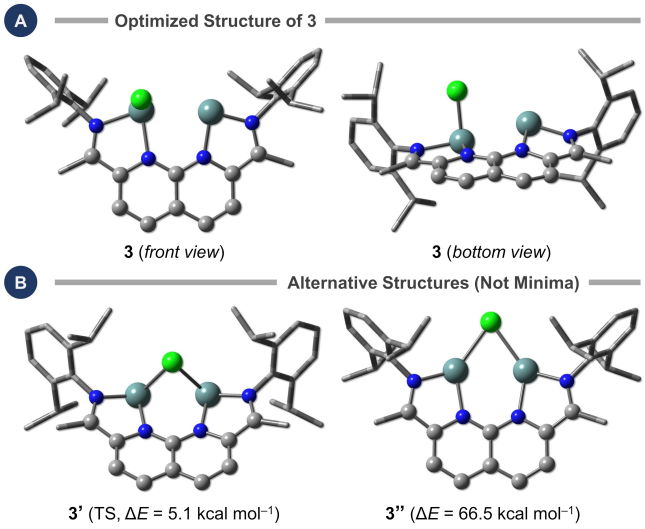

Figure 7. Optimized structures of **3**, **3′**, and **3′′**. Energies ($\triangle E$) are relative to that of **3**. Structure **3′** has an imaginary frequency and is a transition state connecting two enantiomers of **3**. Structure **3′′** is located 61.4 kcal mol^{-1} above **3′**. Hydrogen atoms are omitted for clarity. Level of theory: M06-D3/def2-SVP.

The reaction between one equivalent of Na[BAr$^F_4$] and **1** in benzene proceeded smoothly at ambient temperature, resulting in a red-violet solution. Despite several attempts to optimize the recrystallization conditions or to employ different counteranions, all efforts to obtain crystallographic-grade single crystals proved unsuccessful. However, high-resolution mass spectrometry (HRMS) at m/z = 713.1662 confirmed the successful removal of one chlorine anion (Scheme 2). The attempt to remove the second chlorine atom resulted in decomposition at 130 °C.

In the ^{1}H NMR spectrum of **3**, we observed signals corresponding to the naphthyridine protons at 6.81 and 6.28 ppm, exhibiting a downfield shift compared to those of **1** (6.16 and 5.38 ppm),[5] in line with the electron-deficient nature of the cation. Notably, the difference between the two signals in **3** decreased to 0.53 ppm, compared to 0.78 ppm in **1**. Additionally, a single peak was observed at 2.33 ppm with an integration of four, corresponding to the C*H*Me$_2$ group (Figure S1). This prompted us to explore the possibility of a structure featuring a bridging chloride, as such a motif has been reported in the literature, specifically in the bis-germylene [(MeCNDipp)$_2$C=CHGe}$_2$(μ-Cl)].[4]

In the absence of an experimental crystal structure, we used DFT calculations to investigate the potential structures of compound **3** (Figure 7) and determine their NMR data, the latter computed at the ωB97X–D3/pcSseg-2 level of theory.[14] Our theoretical investigation revealed a structure (**3′**, Figure 7B) featuring a bridging chloride positioned in a bent arrangement relative to the naphthyridine ligand. However, this structure exhibited an imaginary frequency of 98*i* cm^{-1}, indicating that it

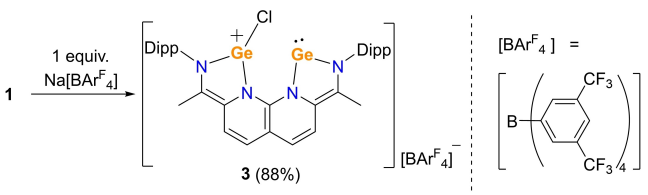

Scheme 2. Synthesis of compound **3** (Dipp = 2,6-diisopropylphenyl).

is not a viable minimum energy structure but rather a transition state (TS).

Additionally, a second structure (**3′′**, Figure 7B) featuring a bridging chloride in a quasi-planar orientation was obtained through constrained optimization. This geometry was significantly less energetically favorable, being located at an energy level 61.4 kcal mol^{-1} higher than that of **3′**. Further examination with various functionals consistently indicated the absence of any minimum energy structure with a bridging chloride.

Following the direction of the imaginary mode of **3′**, we identified a plausible structure for **3** (Figure 7A), wherein the chloride is bound to only one of the germanium centers. The computational analysis of the chemical shifts for this structure revealed that the average deviation of the chemical shifts for the four C*H*Me$_2$ signals was merely 0.34 ppm, which could explain the appearance of a single peak for these protons in the experimental spectrum.

To gain deeper insight into the electronic structure of **3**, we conducted a computational investigation of its electronic absorption features. For this purpose, time-dependent DFT (TD-DFT) calculations were performed at the ωB97X–D3(BJ)/def2-SVPD level of theory,[15] with the results shown in Figure 8. Our calculations reveal that, unlike systems **1** and **2**, where the $S_0 \rightarrow S_1$ transitions occur in the near-infrared region (815 nm and 893 nm, respectively, see Figures S11–S12 in the SI), the corresponding transition in **3** is observed at 578 nm (Figure 8A).

Analysis of the natural transition orbitals (NTOs,[16] Figure 8B) of **3** indicates that this transition is characterized as a $\pi \rightarrow \pi^*$ excitation. The hole NTO spans the entire π framework of the molecule, but is predominantly concentrated in the GeC$_2$N$_2$ ring where Ge is not bound to Cl. In contrast, the electron NTO shows a greater degree of localization in the Ge(Cl)C$_2$N$_2$ ring, including a significant contribution from the Cl atom. These findings suggest that the transition has an appreciable charge

Research Article
doi.org/10.1002/ejic.202400422

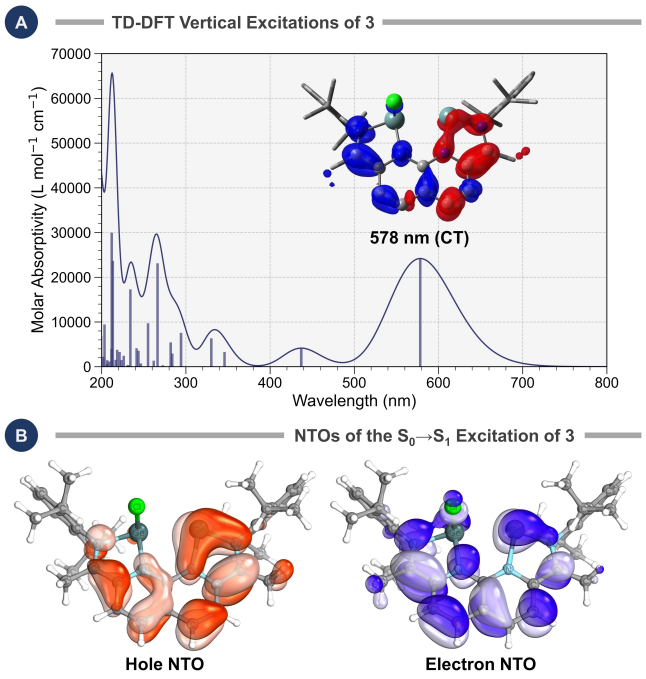

Figure 8. (A) TD-DFT vertical excitations of **3** at the ωB97X–D3(BJ)/def2-SVPD level of theory. The inset figure shows the CDD plot of the $S_0 \rightarrow S_1$ excitation, where the charge flows from red to blue (isovalue: 0.0015). Hydrogen atoms are omitted for clarity. (B) NTOs of the $S_0 \rightarrow S_1$ excitation of **3**.

transfer (CT) character, which is blueshifted relative to compounds **1** and **2** due to the asymmetry of the GeC_2N_2 rings.

The CT character is further supported by the charge density difference (CDD) plot (Figure 8A) and the interfragment charge transfer (IFCT) method, as implemented in Multiwfn 3.8.[17] The CDD plot clearly shows electron flow from the GeC_2N_2 ring to the $Ge(Cl)C_2N_2$ ring. The IFCT analysis quantifies this charge transfer, showing 72.5% CT character, with the GeC_2N_2 ring losing 38.8% of its electron density during excitation, while the $Ge(Cl)C_2N_2$ ring gains 32.6% and the remainder of the molecule gains 6.2%.

These combined results not only explain the red-violet color of compound **3**, consistent with its absorption maximum at 578 nm, but also support the placement of the Cl atom as a terminal ligand rather than a bridging one.

Our calculations confirmed that **3** exhibits only one Ge–Cl single bond, with a characteristic bond length of 2.245 Å. A distance of 3.393 Å between the chloride and the uncoordinated Ge atom ruled out the possibility of chloride bridging. Furthermore, bonding analyses based on the intrinsic bond orbital (IBO)[18] and natural bond orbital (NBO)[19] methods provided no evidence of chloride bonding to the uncoordinated Ge atom. Second-order perturbation energies from NBO calculations indicated the presence of a weak hyperconjugative effect of 6.68 kcal mol^{-1} between the chloride and the uncoordinated Ge atom. However, given the relatively flat potential energy surface concerning the position of the chloride, as evidenced by **3'** being merely 5.1 kcal mol^{-1} above **3**, we cannot rule out the possibility of a fluxional structure. Further investigation is warranted to explore this aspect.

For the reaction between **1** and two equivalents of Li[HB(*s*Bu)$_3$] in C_6D_6, the in situ ^{1}H NMR spectrum indicates the generation of **V** and an unsymmetrical compound species which features four doublets at 5.11, 5.42, 5.94, and 6.13 ppm (Figure S5). Moreover, the singlet at 8.01 ppm is comparable to that of [{HC-(CMeNAr)$_2$}GeH] (Ar = 2,6-*i*Pr$_2$C$_6$H$_3$) (8.08 ppm),[20] implying that hydrido-germylene **4** is a possible intermediate. A prolonged reaction time or removal of the solvent led to the generation of **5** as the major product (Scheme 3).

X-ray diffraction analysis (Figure 9) revealed that the three annulated rings within compound **5** adopt a coplanar arrangement. The largest deviation from the mean plane defined by these rings is only 0.062 Å, attributed to the Ge atom. The coordination-free half of **5**, denoted **5(free)**, resembles the free ligand **IV**. In contrast, the germanium-containing half of **5**, denoted as **5(Ge)**, is similar to compound **V**. The bond distances of compounds **1**, **2**, **5**, **IV**, and **V** suggest that increasing the degree of ligand reduction leads to a shortening of the C_{imine}–C_{Np} bonds, along with a lengthening of the C_{Np}–N_{Np} and N_{imine}–C_{imine} bonds (Figure 10). This trend correlates with observations from Uyeda's study involving dinuclear nickel complexes of NDI.[21]

Conclusions

In conclusion, we have investigated the reactivity of **1**, a dichloro-bis(germylene) compound incorporating a naphthyridine-diimine (NDI) ligand. The reaction with oxidant

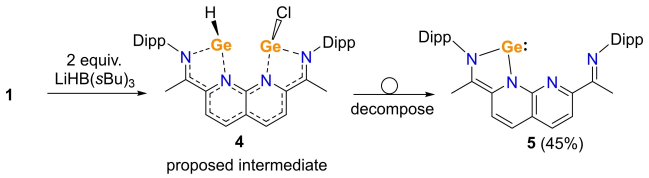

Scheme 3. Synthesis of compound **5** (Dipp = 2,6-diisopropylphenyl).

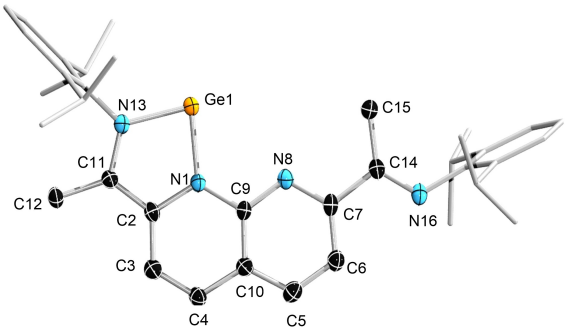

Figure 9. Solid-state structure of **5** (hydrogen atoms and ellipsoids of the Dipp groups are omitted for clarity). Thermal ellipsoids are set at the 50% probability level. Selected bond lengths [Å] and angles [°]: Ge1–N1, 1.8925(17); Ge1–N13, 1.8777(17); N1–C2, 1.409(3); C2–C11, 1.371(3); C11–N13, 1.387(3); C3-C4, 1.347(3); N8–C7, 1.346(3); C7–C14, 1.500(3); C14–N16, 1.277(3); N1–Ge1–N13, 81.91(7); N1–C2–C11, 113.42(18); C2–C11–N13, 112.93(18); C2–N1–C9, 120.09(17); C2–C3–C4, 121.14(19); N8–C7–C14, 117.00(19); C7–C14–N16 115.6(2); C7–N8–C9, 117.58(18); C5–C6–C7, 118.6(2).

Research Article
doi.org/10.1002/ejic.202400422

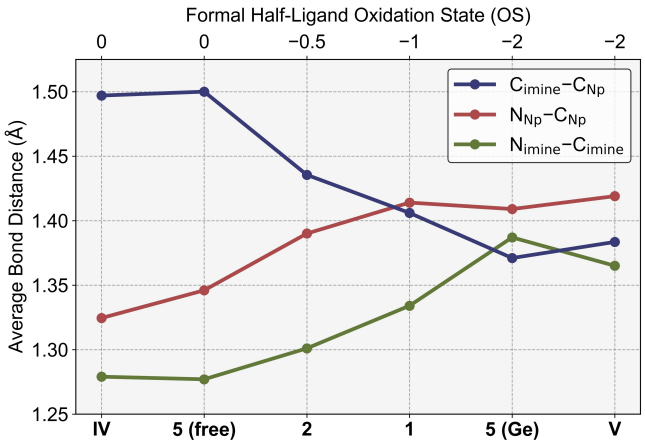

Figure 10. Average bond distances (Å) of the N_{imine}–C_{imine}–C_{Np}–N_{Np} moieties of compounds **IV**, **5**, **2**, **1**, and **V**. The coordination-free and germanium-containing parts of **5** are denoted as **5(free)** and **5(Ge)**, respectively. The estimated standard deviations are $\leq$0.006 Å for all structures. Data are derived from Table S2.

$[Cp_2Fe][BAr^F_4]$ led to the formation of radical species **2**. Moreover, addition of $Na[BAr^F_4]$ to **1** resulted in the abstraction of a single chloride anion, forming compound **3**. When $Li[HB(sBu)_3]$ was used as a hydride source, in-situ ^1H NMR spectroscopy provided evidence for the generation of a mixed hydrido/chlorido bis(germylene), which decomposed to the thermally stable monogermanium species **5**.

Acknowledgements

Financial support from the Julius-Maximilians-University of Würzburg is gratefully acknowledged. Y.H. and J.C. thank the Postgraduate Innovation Foundation of the Wuhan Institute of Technology (No. CX2024340), the Open/Innovation Project of the Engineering Research Center of Phosphorus Resources Development and Utilization of the Ministry of Education (LCX202202), and the Hubei Three Gorges Laboratory (SC240003) for financial support. This work was supported by the Engineering and Physical Sciences Research Council (grant number EP/W52461X/1). This article is also based upon work from the COST Action CA20129 MultIChem, supported by COST (European Cooperation in Science and Technology).

Conflict of Interests

The authors declare no conflict of interest.

Data Availability Statement

The data that support the findings of this study are available from the corresponding author upon reasonable request.

Keywords: Single-electron oxidation · Chloride abstraction · Bis-germylene · Radical cation

[1] a) M. Asay, C. Jones, M. Driess, *Chem. Rev.* **2011**, *111*, 354–396; b) M. Walewska, J. Baumgartner, C. Marschner, L. Albers, T. Müller, *Chem. Eur. J.* **2016**, *22*, 18512–18521; c) M. Walewska, J. Hlina, J. Baumgartner, T. Müller, C. Marschner, *Organometallics* **2016**, *35*, 2728–2737; d) H. Wang, Z. Xie, *Eur. J. Inorg. Chem.* **2017**, *2017*, 4430–4435; e) N. Del Rio, M. Lopez-Reyes, A. Baceiredo, N. Saffon-Merceron, D. Lutters, T. Müller, T. Kato, *Angew. Chem. Int. Ed.* **2017**, *56*, 1365–1370; f) R. Dasgupta, S. Khan, *in Advances in Organometallic Chemistry*, (Ed: P. J. Pérez), Academic Press, Cambridge, **2020**, *74*, 105–152; g) J. A. Cabeza, P. García-Álvarez, C. J. Laglera-Gándara, *Eur. J. Inorg. Chem.* **2020**, *2020*, 784–795; h) R. J. Somerville, J. Campos, *Eur. J. Inorg. Chem.* **2021**, *2021*, 3488–3498. i) M. Ghosh, N. Sen, S. Khan, *ACS Omega* **2022**, *7*, 6449–6454; j) V. Y. Lee, *Eur. J. Inorg. Chem.* **2022**, *2022*, e202200175; k) Y. Qin, Y. Kang, L. Zhang, J. Sun, Z. Zhang, J. Xu, F. Zeng, A. Li, W. Wang, W. Shi, *Chin. J. Chem.* **2023**, *35*, 108691–108694; l) K. V. Arsenyeva, A. V. Piskunov, *J. Struct. Chem.* **2023**, *64*, 1–45.
[2] a) Y. N. Lebedev, U. Das, G. Schnakenburg, A. C. Filippou, *Organometallics* **2017**, *36*, 1530–1540; b) A. Schulz, T. L. Kalkuhl, P. M. Keil, T. J. Hadlington, *Angew. Chem. Int. Ed.*, **2023**, *62*, e202305996; c) A. F. Richards, A. D. Phillips, M. M. Olmstead, P. P. Power, *J. Am. Chem. Soc.* **2003**, *125*, 3204–3205.
[3] a) Y. Li, K. C. Mondal, P. Stollberg, H. Zhu, H. W. Roesky, R. Herbst-Irmer, D. Stalke, H. Fliegl, *Chem. Commun.* **2014**, *50*, 3356–3358; b) Y. Su, Y. Li, R. Ganguly, R. Kinjo, *Eur. J. Inorg. Chem.* **2018**, *2018*, 2228–2231; c) X. Gao, Y. He, J. Cui, *J. Organomet. Chem.* **2024**, *1012*, 123146–123162.
[4] E. Hupf, F. Kaiser, P. A. Lummis, M. M. D. Roy, R. McDonald, M. J. Ferguson, F. E. Kühn, E. Rivard, *Inorg. Chem.* **2020**, *59*, 1592–1601.
[5] J. Cui, J. Weiser, F. Fantuzzi, M. Dietz, Y. Yatsenko, A. Hafner, S. Nees, I. Krummenacher, M. Zhang, K. Hammond, P. Roth, W. Lu, R. D. Dewhurst, B. Engels, H. Braunschweig, *Chem. Commun.* **2022**, *58*, 13357–13360.
[6] Deposition Number(s) 2278647 (for 2) and 2312125 (for 5)contain(s) the supplementary crystallographic data for this paper. These data are provided free of charge by the joint Cambridge Crystallographic Data Centre and Fachinformationszentrum Karlsruhe Access Structures service.
[7] a) Y. Zhao, D. G. Truhlar, *Theor. Chem. Acc.* **2008**, *120*, 215–241; b) S. Grimme, J. Antony, S. Ehrlich, H. Krieg, *J. Chem. Phys.* **2010**, *132*, 154104; c) F. Weigend, R. Ahlrichs, *Phys. Chem. Chem. Phys.* **2005**, *7*, 3297–3305.
[8] J. Weiser, J. Cui, R. D. Dewhurst, H. Braunschweig, B. Engels, F. Fantuzzi, *J. Comput. Chem.* **2023**, *44*, 456–467.
[9] I. L. Fedushkin, N. M. Khvoinova, A. Y. Baurin, G. K. Fukin, V. K. Cherkasov, M. P. Bubnov, *Inorg. Chem.* **2004**, *43*, 7807–7815.
[10] S.-P. Chia, E. Carter, H.-W. Xi, Y. Li, C.-W. So, *Angew. Chem. Int. Ed.* **2014**, *53*, 8455–8458.
[11] X. Lu, H. Cheng, Y. Meng, X. Wang, L. Hou, Z. Wang, S. Chen, Y. Wang, G. Tan, A. Li, W. Wang, *Organometallics* **2017**, *36*, 2706–2709.
[12] Y. Dai, M. Bao, W. Wang, Z. Xie, C. Liu, Y. Su, *Chinese J. Chem.* **2022**, *40*, 2387–2392.
[13] T. Kodama, K. Uchida, C. Nakasuji, R. Kishi, Y. Kitagawa, M. Tobisu, *Inorg. Chem.* **2023**, *62*, 7861–7867.
[14] a) Y.-S. Lin, G.-D. Li, S.-P. Mao, J.-D. Chai, *J. Chem. Theory Comput.* **2013**, *9*, 263–272; b) F. Jensen, *J. Chem. Theory Comput.* **2015**, *11*, 132–138.
[15] A. Najibi, L. Goerigk, *J. Chem. Theory Comput.* **2018**, *14*, 5725–5738.
[16] R. L. Martin, *J. Chem. Phys.* **2003**, *118*, 4775–4777.
[17] T. Lu, F. Chen, *J. Comput. Chem.* **2012**, *33*, 580–592.
[18] G. Knizia, *J. Chem. Theory Comput.* **2013**, *9*, 4834–4843.
[19] F. Weinhold, C. R. Landis, E. D. Glendening, *Int. Rev. Phys. Chem.* **2016**, *35*, 399–440.
[20] a) L. W. Pineda, V. Jancik, K. Starke, R. B. Oswald, H. W. Roesky, *Angew. Chem. Int. Ed.* **2006**, *45*, 2602–2605; b) Y. Ding, H. Hao, H. W. Roesky, M. Noltemeyer, H.-G. Schmidt, *Organometallics* **2001**, *20*, 4806–4811.
[21] Y. Y. Zhou, D. R. Hartline, T. J. Steiman, P. E. Fanwick, C. Uyeda, *Inorg. Chem.* **2014**, *53*, 11770–11777.
[22] R. Ditchfield, *Mol. Phys.* **1974**, *27*, 789–807.
[23] K. Wolinski, J. F. Hinton, P. Pulay, *J. Am. Chem. Soc.* **1990**, *112*, 8251–8260.
[24] F. Calderazzo, G. Pampaloni, L. Rocchi, U. Englert, *Organometallics* **1994**, *13*, 2592–2601.
[25] J. R. Cheeseman, G. W. Trucks, T. A. Keith, M. J. Frisch, *J. Chem. Phys.* **1996**, *104*, 5497–5509.
[26] S. Hirata, M. Head-Gordon, *Chem. Phys. Lett.* **1999**, *314*, 291–299.

Research Article
doi.org/10.1002/ejic.202400422

[27] J. Le Bras, H. Jiao, W. E. Meyer, F. Hampel, J. A. Gladysz, *J. Organomet. Chem.* **2000**, *616*, 54–66.
[28] D. L. Reger, T. D. Wright, C. A. Little, J. J. Lamba, M. D. Smith, *Inorg. Chem.* **2001**, *40*, 3810–3814.
[29] M. Cossi, N. Rega, G. Scalmani, V. Barone, *J. Comput. Chem.* **2003**, *24*, 669–681.
[30] F. Neese, *J. Comput. Chem.* **2003**, *24*, 1740–1747.
[31] G. M. Sheldrick, *Acta Cryst.* **2008**, *A64*, 112–122.
[32] F. Neese, F. Wennmohs, A. Hansen, U. Becker, *Chem. Phys.* **2009**, *356*, 98–109.
[33] F. Neese, *Wiley Interdiscip. Rev. Comput. Mol. Sci.* **2012**, *2*, 73–78.
[34] G. M. Sheldrick, *Acta Cryst.* **2015**, *A71*, 3–8.
[35] A. L. Spek, *Acta Crystallogr. C Struct. Chem.* **2015**, *71*, 9–18.
[36] M. J. Frisch, G. W. Trucks, H. B. Schlegel, G. E. Scuseria, M. A. Robb,J. R. Cheeseman, G. Scalmani, V. Barone, G. A. Petersson, H. Nakatsuji, X. Li, M. Caricato, A. V. Marenich, J. Bloino, B. G. Janesko, R. Gomperts, B. Mennucci, H. P. Hratchian, J. V. Ortiz, A. F. Izmaylov, J. L. Sonnenberg, Williams, F. Ding, F. Lipparini, F. Egidi, J. Goings, B. Peng, A. Petrone, T. Henderson, D. Ranasinghe, V. G. Zakrzewski, J. Gao, N. Rega, G. Zheng, W. Liang, M. Hada, M. Ehara, K. Toyota, R. Fukuda, J. Hasegawa, M. Ishida, T. Nakajima, Y. Honda, O. Kitao, H. Nakai, T. Vreven, K. Throssell, J. A. Montgomery Jr., J. E. Peralta, F. Ogliaro, M. J. Bearpark, J. J. Heyd, E. N. Brothers, K. N. Kudin, V. N. Staroverov, T. A. Keith, R. Kobayashi, J. Normand, K. Raghavachari, A. P. Rendell, J. C. Burant, S. S. Iyengar, J. Tomasi, M. Cossi, J. M. Millam, M. Klene, C. Adamo, R. Cammi, J. W. Ochterski, R. L. Martin, K. Morokuma, O. Farkas, J. B. Foresman, D. J. Fox, *Gaussian 16, Revision C.01*, Gaussian, Inc., Wallingford, CT **2016**.
[37] W. J. Kerr, R. J. Mudd, J. A. Brown, *Chem. Eur. J.* **2016**, *22*, 4738–4742.
[38] F. Neese, *WIREs Comput. Mol. Sci.* **2022**, *12*, e1606.

Manuscript received: July 3, 2024
Revised manuscript received: August 23, 2024
Accepted manuscript online: August 23, 2024
Version of record online: October 22, 2024